

Random Coupling of Chaotic Maps leads to Spatiotemporal Synchronisation

Sudeshna Sinha¹

Institute of Mathematical Sciences, Taramani, Chennai 600 113, India

Abstract

We investigate the spatiotemporal dynamics of a network of coupled chaotic maps, with varying degrees of randomness in coupling connections. While strictly nearest neighbour coupling never allows spatiotemporal synchronization in our system, randomly rewiring some of those connections stabilises entire networks at x^* , where x^* is the strongly unstable fixed point solution of the local chaotic map. In fact, the smallest degree of randomness in spatial connections opens up a window of stability for the synchronised fixed point in coupling parameter space. Further, the coupling ϵ_{bif_r} at which the onset of spatiotemporal synchronisation occurs, scales with the fraction of rewired sites p as a power law, for $0.1 < p < 1$. We also show that the regularising effect of random connections can be understood from stability analysis of the probabilistic evolution equation for the system, and approximate analytical expressions for the range and ϵ_{bif_r} are obtained.

1 Introduction

The Coupled Map Lattice (CML) was introduced as a simple model capturing the essential features of nonlinear dynamics of extended systems [1]. Over the past decade research centred around CML has yielded suggestive conceptual models of spatiotemporal phenomena, in fields ranging from biology to engineering. In particular, this class of systems is of considerable interest in modelling phenomena as diverse as josephson junction arrays, multimode lasers, vortex dynamics, and even evolutionary biology. The ubiquity of distributed complex systems has made the CML a focus of sustained research interest.

A very well-studied coupling form in CMLs is nearest neighbour coupling. While this regular network is the chosen topology of innumerable studies, there are strong reasons to re-visit this fundamental issue in the light of the fact that some degree of randomness in spatial coupling can be closer to physical reality than strict nearest neighbour scenarios. In fact many systems of biological, technological and physical significance are better described by randomising some fraction of the regular links [2-7]. So here we will study the spatiotemporal dynamics of CMLs with some of its coupling connections rewired randomly, i.e. an extended system comprised of a collection of elemental dynamical units with varying degrees of randomness in its spatial connections.

¹sudeshna@imsc.ernet.in

Specifically we consider a one-dimensional ring of coupled logistic maps. The sites are denoted by integers $i = 1, \dots, N$, where N is the linear size of the lattice. On each site is defined a continuous state variable denoted by $x_n(i)$, which corresponds to the physical variable of interest. The evolution of this lattice, under standard nearest neighbour interactions, in discrete time n is given by

$$x_{n+1}(i) = (1 - \epsilon)f(x_n(i)) + \frac{\epsilon}{2}\{x_n(i+1) + x_n(i-1)\} \quad (1)$$

The strength of coupling is given by ϵ . The local on-site map is chosen to be the fully chaotic logistic map: $f(x) = 4x(1-x)$. This map has widespread relevance as a prototype of low dimensional chaos.

Now we will consider the above system with its coupling connections rewired randomly in varying degrees, and try to determine what dynamical properties are significantly affected by the way connections are made between elements. In our study, at every update we will connect a fraction p of randomly chosen sites in the lattice, to 2 other random sites, instead of their nearest neighbours as in Eqn. 1. That is, we will replace a fraction p of nearest neighbour links by random connections. The case of $p = 0$ corresponds to the usual nearest neighbour interaction, while $p = 1$, corresponds to completely random coupling [2-7].

This scenario is much like small world networks at low p , namely $p \sim 0.01$. Note however that we explore the full range of p here. In our work $0 \leq p \leq 1$. So the study is inclusive of, but not confined to, small world networks.

2 Numerical Results

We will now present numerical evidence that random rewiring has a pronounced effect on spatiotemporal synchronisation. The numerical results here have been obtained by sampling a large set of random initial conditions ($\sim 10^4$), and with lattice sizes ranging from 10 to 1000.

Figs. 1 and 2 display the state of the network, $x_n(i), i = 1, \dots, N$, with respect to coupling strength ϵ , for the limiting cases of nearest neighbour interactions (i.e. $p = 0$) and completely random coupling (i.e. $p = 1$). It is clearly seen that the standard nearest neighbour coupling does not yield a spatiotemporal fixed point anywhere in the entire coupling range $0 \leq \epsilon \leq 1$ [8].

Now the effect of introducing some random connections, i.e. $p > 0$, is to *create windows in parameter space where a spatiotemporal fixed point state gains stability*, i.e. where one finds all lattice sites synchronised at $x_n(i) = x^* = 3/4$, for all sites i and at all times n . Note that $x^* = f(x^*)$ is the fixed point solution of the individual chaotic maps, and is strongly unstable in the local chaotic map. We then have for all $p > 0$, a stable region of synchronised fixed points in the parameter interval: $\epsilon_{bifr} \leq \epsilon \leq 1.0$. The value of ϵ_{bifr} , where the

spatiotemporally invariant state onsets, is dependent on p . It is evident from Fig. 2 that ϵ_{bif_r} for completely random coupling $p = 1$ is around 0.62.

The relationship between the fraction of rewired connections p and the range, $\mathcal{R} = (1 - \epsilon_{bif_r})$, within which spatiotemporal homogeneity is obtained, is displayed in Fig. 3. It is clearly evident that unlike nearest neighbour coupling, random coupling leads to large parameter regimes of regular homogeneous behaviour, with all lattice sites synchronised exactly at $x(i) = x^* = 0.75$. Furthermore the synchronised spatiotemporal fixed point gains stability over some finite parameter range under *any* finite p , i.e. whenever $p > 0$, however small, we have $\mathcal{R} > 0$. In that sense strictly nearest neighbour coupling is singular as it does not support spatiotemporal synchronisation anywhere in coupling parameter space, whereas any degree of randomness in spatial coupling connections opens up a synchronised fixed point window. Thus random connections yield spatiotemporal homogeneity here, while completely regular connections never do.

The relationship between ϵ_{bif_r} , the point of onset of the spatiotemporal fixed phase, and p is shown in Fig. 4. Note that for $p < 0.1$ random rewiring does not affect ϵ_{bif_r} much. Only after $p \sim 0.1$ does ϵ_{bif_r} fall appreciably. Further, it is clearly evident that for $0.1 < p \leq 1$ the lower end of the stability range falls with increasing p as a well defined power law. Note that lattice size has very little effect on ϵ_{bif_r} , and the numerically obtained ϵ_{bif_r} for ensembles of initial random initial conditions over a range of lattice sizes $N = 10, 50, 100$ and 500 fall quite indistinguishably around each other.

The robust spatiotemporal fixed point supported by random coupling may have significant ramifications. It has immediate relevance to the important problem of controlling/synchronising extended chaotic systems [10, 11]. Obtaining spatiotemporal synchronisation by introducing some random spatial connections may have practical utility in the control of large interactive systems. The regularising effect of random coupling may then help to devise control methods for spatially extended interactive systems, as well as suggest natural regularising mechanisms in physical and biological systems.

3 Analytical Results

We shall now analyse this system to account for the much enhanced stability of the homogeneous phase under random connections. The only possible solution for a spatiotemporally synchronized state here is one where all $x_n(i) = x^*$, and $x^* = f(x^*)$ is the fixed point solution of the local map. For the case of the logistic map $x^* = 4x^*(1 - x^*) = 3/4$.

To calculate the stability of the lattice with all sites at x^* we will construct an *average probabilistic evolution rule* for the sites, which becomes a sort of *mean field version of the dynamics*. Some effects due to fluctuations are lost, but as a first approximation we have found this approach qualitatively right,

and quantitatively close to to the numerical results as well.

We take into account the following: all sites have probability p of being coupled to random sites, and probability $(1-p)$ of being wired to nearest neighbours. Then the averaged evolution equation of a site j is

$$x_{n+1}(j) = (1-\epsilon)f(x_n(j)) + (1-p)\frac{\epsilon}{2}\{x_n(j+1) + x_n(j-1)\} + p\frac{\epsilon}{2}\{x_n(\xi) + x_n(\eta)\} \quad (2)$$

where ξ and η are random integers between 1 and N .

To calculate the stability of the coherent state, we perform the usual linearization. Replacing $x_n(j) = x^* + h_n(j)$, and expanding to first order gives

$$\begin{aligned} h_{n+1}(j) &= (1-\epsilon)f'(x^*)h_n(j) + (1-p)\frac{\epsilon}{2}\{h_n(j+1) + h_n(j-1)\} \\ &\quad + p\frac{\epsilon}{2}\{h_n(\xi) + h_n(\eta)\} \\ &\approx (1-\epsilon)f'(x^*)h_n(j) + (1-p)\frac{\epsilon}{2}\{h_n(j+1) + h_n(j-1)\} \end{aligned} \quad (3)$$

as to a first approximation one can consider the sum over the fluctuations of the random neighbours to be zero. This approximation is clearly more valid for small p .

For stability considerations one can diagonalize the above expression using a Fourier transform ($h_n(j) = \sum_q \phi_n(q) \exp(ijq)$, where q is the wavenumber and j is the site index), which finally leads us to the following growth equation:

$$\frac{\phi_{n+1}}{\phi_n} = f'(x^*)(1-\epsilon) + \epsilon(1-p)\cos q \quad (4)$$

with q going from 0 to π . Clearly the stabilisation condition will depend on the nature of the local map $f(x)$ through the term $f'(x)$ in Eqn. 4. Considering the fully chaotic logistic map with $f'(x^*) = -2$, one finds that the growth coefficient that appears in this formula is smaller than one in magnitude if and only if

$$\frac{1}{1+p} < \epsilon < 1 \quad (5)$$

i.e.

$$\epsilon_{bifur} = \frac{1}{1+p} \quad (6)$$

and the range of stability \mathcal{R} is

$$\mathcal{R} = 1 - \frac{1}{1+p} = \frac{p}{1+p} \quad (7)$$

For small p ($p \ll 1$) standard expansion gives

$$\mathcal{R} \sim p \quad (8)$$

The usual case of regular nearest neighbour couplings, $p = 0$, gives a null range, as the upper and lower limits of the range coincide. When all connections are random, i.e. $p = 1$ the largest stable range is obtained, and the lower end of the stable window ϵ_{bifr} is minimum, with $\epsilon_{bifr} = 1/2$. So stability analysis also clearly dictates that enhanced stability of the homogeneous phase must occur under random connections, just as numerical evidence shows.

Fig. 3 exhibits both the analytical expression of Eq.(7) and the numerically obtained points for comparison. It is clear that for small p the numerically obtained $\mathcal{R} \sim p$ is in complete agreement with the analytical formula. But for higher p some deviation is discernable, as the ignored effect of the fluctuating contributions from random neighbours is weighted by p , and hence more pronounced for large p . Here the numerically obtained result goes as

$$\epsilon_{bifr} \sim p^{-\phi} \quad (9)$$

for $0.1 < p \leq 1$, with $\phi \sim 0.2$ (see Figs. 4 and 7).

Note that when $p < 0.1$ the effect on ϵ_{bifr} is not significant. Only when $0.1 < p \leq 1$ does ϵ_{bifr} fall appreciably. So connecting elements in a small world network is not sufficient to make much difference to the onset of the stable spatiotemporally synchronised state [9].

4 Results from Other Models

In order to examine the range of applicability of this phenomena we have examined coupled tent maps and coupled sine circle maps as well. In the case of coupled tent maps the local map in Eqn. 1 is given as

$$f(x) = 1 - 2|x - 1/2| \quad (10)$$

The tent map has an unstable fixed point at $x^* = 2/3$, with local slope $f'(x^*) = -2$. For coupled circle map networks the local map in Eqn. 1 is given as

$$f = x + \Omega - \frac{K}{2\pi} \sin(2\pi x) \quad (11)$$

and Eqn. 1 is taken *mod* 1. In the representative example chosen here the parameters of the circle map are $\Omega = 0, K = 3$. Here too the local map has a strongly unstable fixed point at $x^* = \frac{1}{2\pi} \sin^{-1}(\Omega/K)$, with $f'(x^*) = -2$. Numerics very clearly show that both these systems yield the same phenomena as logistic maps, namely, one obtains a stable range for spatiotemporal synchronisation on random rewiring (see Figs. 5 and 6 for the limiting cases of $p = 0$ and $p = 1$ in coupled circle maps).

Since the $f'(x^*)$ of both the tent map and the circle map above is -2 , we expect from our analysis (Eqn. 4) that their ϵ_{bifr} and \mathcal{R} will be the same as for logistic maps. This is indeed exactly true, as is evident from Fig. 7 which

displays the point of onset of spatiotemporal synchronisation for all three cases. In fact the numerically obtained ϵ_{bifr} values for ensembles of coupled tent, circle and logistic maps fall indistinguishably around each other, even for high p where Eqn. 4 is expected to be less accurate.

Additionally one can infer from the stability analysis above, how strongly unstable the local maps can possibly be while still allowing random connections to stabilise the spatiotemporal fixed point. From Eqn. 4 it follows that the onset of spatiotemporal regularity is governed by the condition

$$|f'(x^*)| < \frac{1 - \epsilon + \epsilon p}{1 - \epsilon} = 1 + \frac{\epsilon p}{1 - \epsilon} \quad (12)$$

Clearly then, locally unstable maps with $|f'(x^*)| > 1$ can be stabilised by any finite p , i.e. by any degree of randomness in the coupling connections. As coupling strength ϵ and fraction of rewiring p increases, maps with increasingly unstable fixed points can be synchronised stably by random rewiring. For regular coupling ($p = 0$) on the other hand the local instability can only be as large as 1, i.e. if and only if the local components possess stable fixed points can their network be stabilised at spatiotemporal fixed points, as numerics have already shown.

Lastly, in certain contexts, especially neuronal scenarios, the randomness in coupling may be *static*. In the presence of such quenched randomness in the couplings, once again one obtains a stable range \mathcal{R} for spatiotemporal synchronisation. But unlike dynamical rewiring where the \mathcal{R} is independent of the size and initial preparation of the lattice and its connections, here there is a spread in the values of \mathcal{R} obtained from different (static) realisations of the random connections. Furthermore, this distribution of \mathcal{R} is dependent on the size of network. For instance, on an average, networks of size $N = 10$ with fully random static connections ($p = 1$) yield $\epsilon_{bifr} \sim 0.75$ and those of size $N = 100$ yield $\epsilon_{bifr} \sim 0.85$, as opposed to $\epsilon_{bifr} \sim 0.62$ obtained for all N for dynamically updated random connections. Fig. 8 displays the average range $\langle \mathcal{R} \rangle$ with respect to network size N , indicative of clear scaling behaviour:

$$\langle \mathcal{R} \rangle \sim N^{-\nu} \quad (13)$$

with $\nu \sim 0.24$. This suggests that the range narrows *slowly* with increasing network size. So, while in the limit of infinite lattices there will be no spatiotemporal synchronisation, for finite networks static randomness will lead to stable windows of spatiotemporal synchronisation.

This behaviour can be understood by examining the linear stability of the homogeneous solution: $x_n(j) = x^*$ for all sites j at all times n . For instance for the case of fully random static connections $p = 1$, considering the dynamics of small perturbations over the network one obtains the transfer matrix connecting the perturbation vectors at successive times to be a sum of a $N \times N$ diagonal matrix, with entries $(1 - \epsilon)f'(x^*)$, and $\epsilon/2 \times \mathbf{C}$ where \mathbf{C} is a $N \times N$ sparse

non-symmetric matrix with two random entries of 1 on each row. Now the minimum of the real part of the eigenvalues of \mathbf{C} , λ_{\min} , crucially governs the stability. Typically $\epsilon_{bifur} = 2/\{\lambda_{\min} + 4\}$ when $f'(x^*) = -2$. Now the values of λ_{\min} obtained from different static realisations of the connectivity matrix \mathbf{C} are distributed differently for different sizes N . For small N this distribution is broad and has less negative averages (~ -1). On the other hand for large N the distribution gets narrower and tends towards the limiting value of -2 . This results in a larger range of stability, and greater spread in ϵ_{bifur} for small networks. In fact for small N , certain static realisations yield a larger range of stability ($\mathcal{R} \sim 1/2$) than dynamic rewiring.

5 Conclusions

In summary then, we have shown that random rewiring of spatial connections has a pronounced effect on spatiotemporal synchronisation. In fact strictly nearest neighbour coupling is not generic, in that it does not support any spatiotemporal fixed point phase, while the smallest degree of random rewiring has the effect of creating a window of spatiotemporal invariance in coupling parameter space. Further the regularising effect of random connections can be understood from stability analysis of the probabilistic evolution equation for the system, and approximate analytical expressions for the range and onset of spatiotemporal synchronisation have been obtained. The key observation that *random coupling regularises* may then help to devise control methods for spatially extended interactive systems, as well as suggest natural regularising mechanisms in physical and biological systems.

Acknowledgements: I would like to thank Neelima Gupte for many stimulating discussions and ideas on the subject.

References

- [1] K. Kaneko, ed. *Theory and Applications of Coupled Map Lattices*, (Wiley, 1993); J. Crutchfield and K. Kaneko, in *Directions in Chaos*, edited by Hao Bai-Lin (1987, World Scientific, Singapore) and references therein.
- [2] Watts, D.J. and Strogatz, Nature (London) **393** (1998) 440; Collins, J.J. and Chow, C.C. Nature (London) **393** (1998) 409.
- [3] Hopfield, J.J. and Hertz, A.V.M., Proc. Natl. Acad. Sci. USA **92** (1995) 6655.
- [4] Pandit, S.A. and Amritkar, R.E., Phys. Rev. E **60** (1999) R1119; Phys. Rev. E **63** (2001) 041104.

- [5] Christiansen, K. *et al*, Phys. Rev. Letts. **81** (1998) 2380.
- [6] Barthelemy, M. and Nunes Amaral, L.A., Phys. Rev. letts. **82** (1999) 3180.
- [7] Bagnoli F. and Cecconi, F., Phys. Letts. A **282** (2001) 9.
- [8] Only the strong coupling range $1/2 \leq \epsilon \leq 1$ is displayed in Figs. 1 and 2. The weak coupling range $0 \leq \epsilon \leq 1/2$ (not shown) is strongly irregular for both $p = 0$ and $p = 1$.
- [9] The range of stability also depends on the specific coupling form: for instance if one considered the future-coupled case, where the coupling occurs through $f(x)$ then an additional factor of $f'(x)$ multiplies the second term in Eqn. 4. The validity of the approximation in Eqn. 3 also depends on the coupling form. Again for the future-coupled case the approximation is much worse as the term ignored is weighted by an additional factor of $f'(x)$, which is greater than 1 for chaotic maps. In fact for the future-coupled case numerical evidence of spatial synchronisation is obtained for chaotic logistic maps with $f(x) = rx(1 - x)$, only when $r < 4$, e.g. around $r \sim 3.8$. But even for $r \sim 4$, where exact synchronisation is not obtained, the roughness of the spatial profile is much less than that for regular nearest neighbour coupling. So the random coupling does have a regularising effect there as well, though not as complete as in the examples in this work.
- [10] Ditto, W.L. *et al*, Nature **376** (1995) 465; Sinha, S. and Gupte, N. Phys. Rev. E **58** (1998) R5221-5224; Phys. Rev. E **64** (2001) R015203-015206.
- [11] Some references of this rapidly growing field of interest are: L. Pecora and T.M. Caroll, Phys. Rev. Letts., **64** (1990) 821; Phys. Rev. A **44** (1991) 2374; T.L. Caroll, Phys. Rev. E **50** (1994) 2580; F. Heagy, T.L. Caroll and L.M. Pecora, Phys. Rev. E **50** (1994) 1874; D. Auerbach, Phys. Rev. Letts. **72** (1994) 1184.

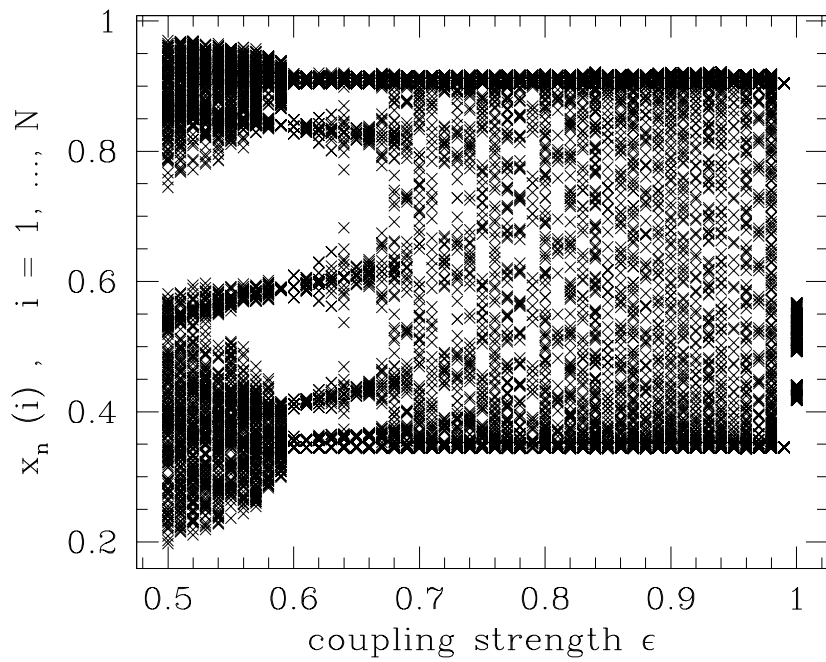


Figure 1: Bifurcation diagram showing values of $x_n(i)$ with respect to coupling strength ϵ , for coupled logistic maps with strictly regular nearest neighbour connections. Here the linear size of the lattice is $N = 100$ and in the figure we plot $x_n(i)$ ($i = 1, \dots, 100$) over $n = 1, \dots, 5$ iterations (after a transience time of 1000) for 5 different initial conditions.

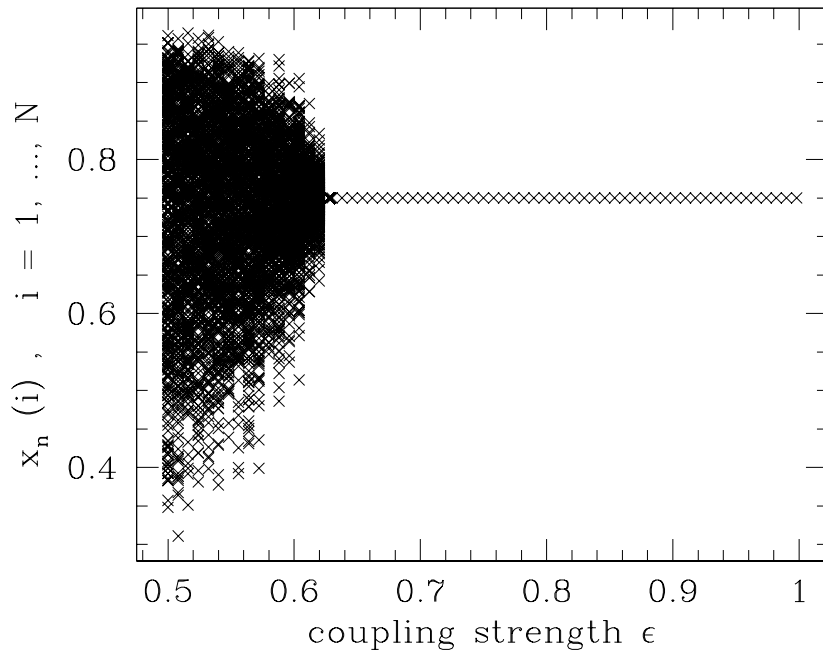


Figure 2: Bifurcation diagram showing values of $x_n(i)$ with respect to coupling strength ϵ , for coupled logistic maps with completely random connections. Here the linear size of the lattice is $N = 100$ and in the figure we plot $x_n(i)$ ($i = 1, \dots, 100$) over $n = 1, \dots, 5$ iterations (after a transience time of 1000) for 5 different initial conditions.

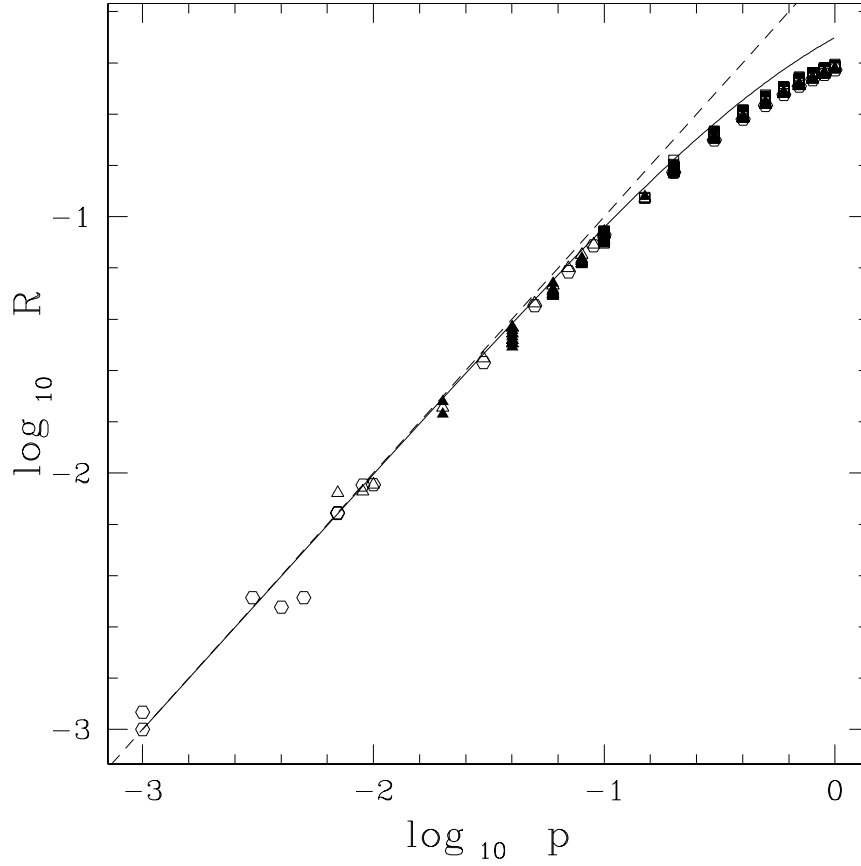


Figure 3: The stable range R with respect to the fraction of randomly rewired sites p ($0.001 \leq p \leq 1$): the solid line displays the analytical result of Eqn. 7, and the different points are obtained from numerical simulations over several different initial conditions, for 4 different lattice sizes, namely $N = 10, 50, 100$ and 500 . The dotted line shows $R = p$, and it is clear that for a large range of p the approximation holds.

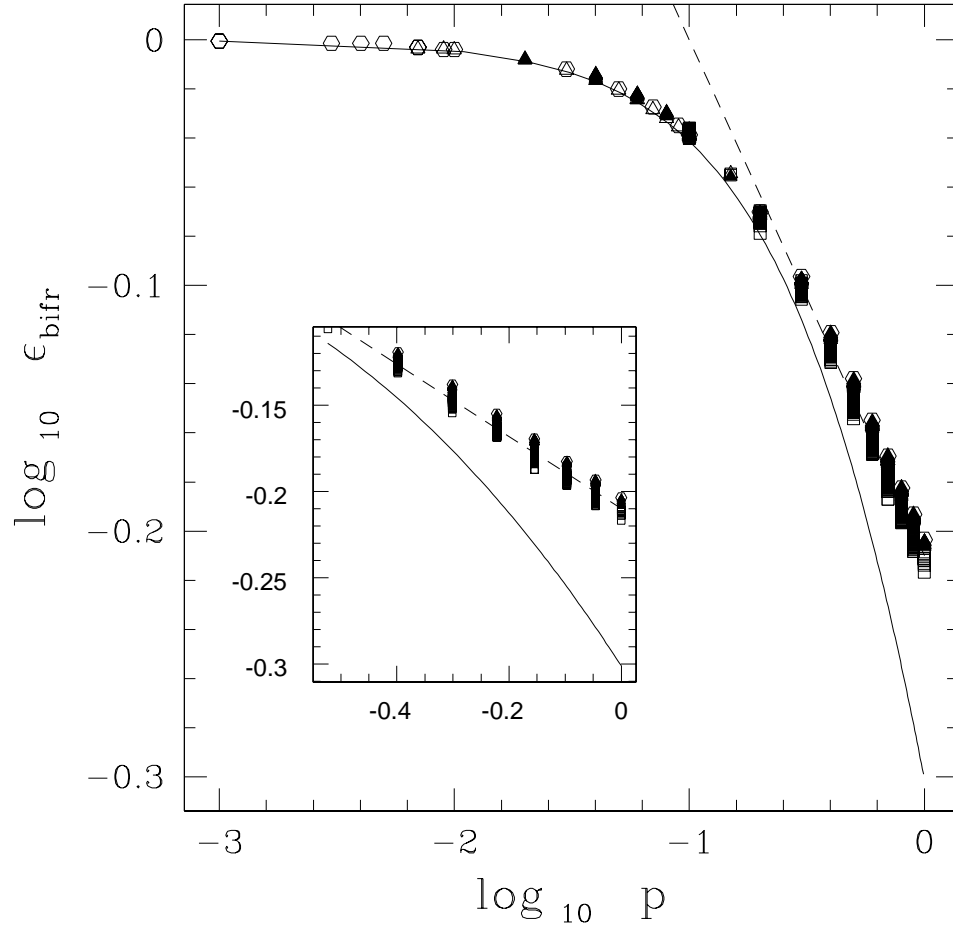


Figure 4: The ϵ_{bifr} (i.e. the value of coupling at which the onset of spatiotemporal synchronization occurs) with respect to fraction of randomly rewired sites p ($0.001 \leq p \leq 1$): the solid line displays the analytical result of Eqn. 6, and the points are obtained from numerical simulations over several different initial conditions, for 4 different lattice sizes, namely $N = 10, 50, 100$ and 500 . The inset box shows a blow-up of $0.1 < p \leq 1$. Here the numerically obtained ϵ_{bifr} deviates from the mean field results. The dashed line is the best fit straight line for the numerically obtained points in that region.

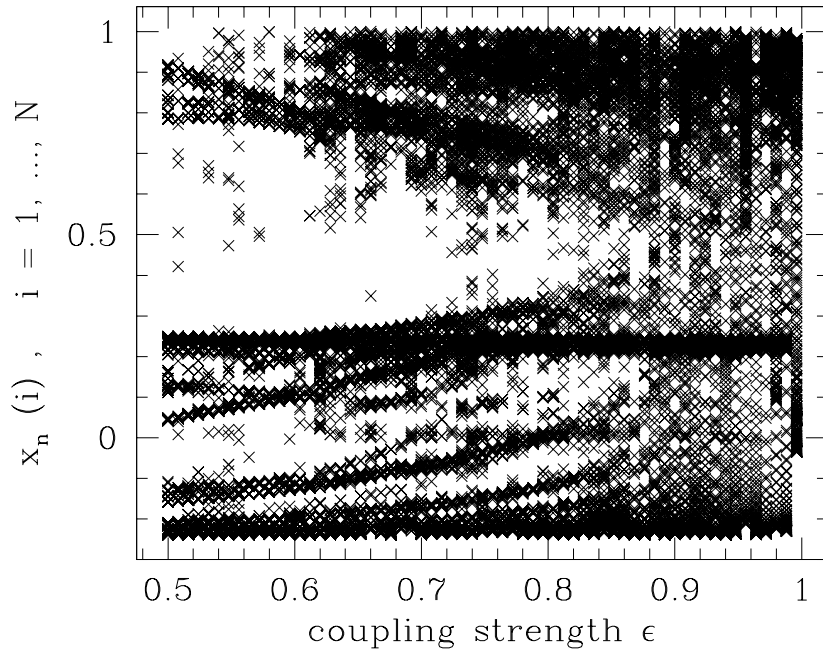


Figure 5: Bifurcation diagram showing values of $x_n(i)$ with respect to coupling strength ϵ , for coupled sine circle maps with strictly regular nearest neighbour connections. Here the linear size of the lattice is $N = 100$ and in the figure we plot $x_n(i)$ ($i = 1, \dots, 100$) over $n = 1, \dots, 5$ iterations (after a transience time of 1000) for 5 different initial conditions.

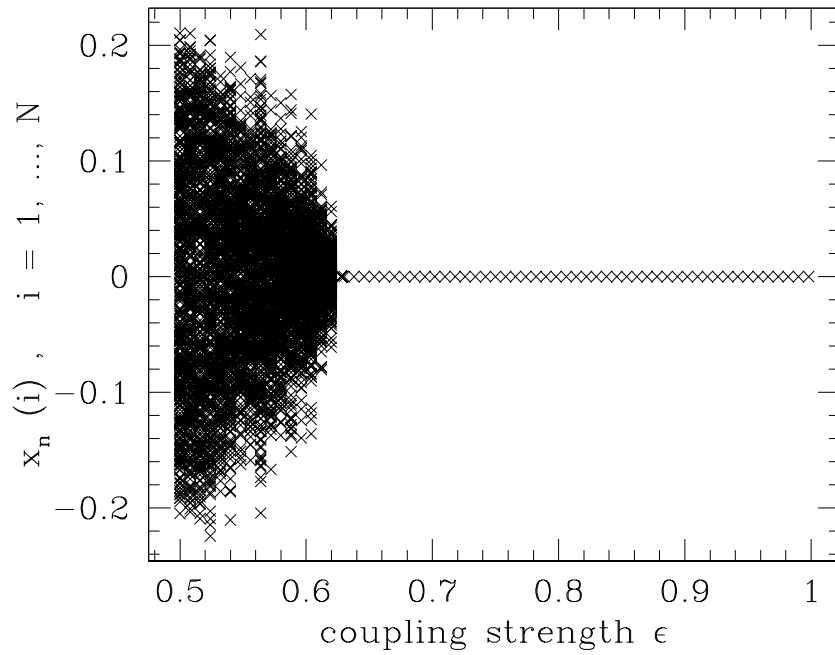


Figure 6: Bifurcation diagram showing values of $x_n(i)$ with respect to coupling strength ϵ , for coupled sine circle maps with completely random connections. Here the linear size of the lattice is $N = 100$ and in the figure we plot $x_n(i)$ ($i = 1, \dots, 100$) over $n = 1, \dots, 5$ iterations (after a transience time of 1000) for 5 different initial conditions.

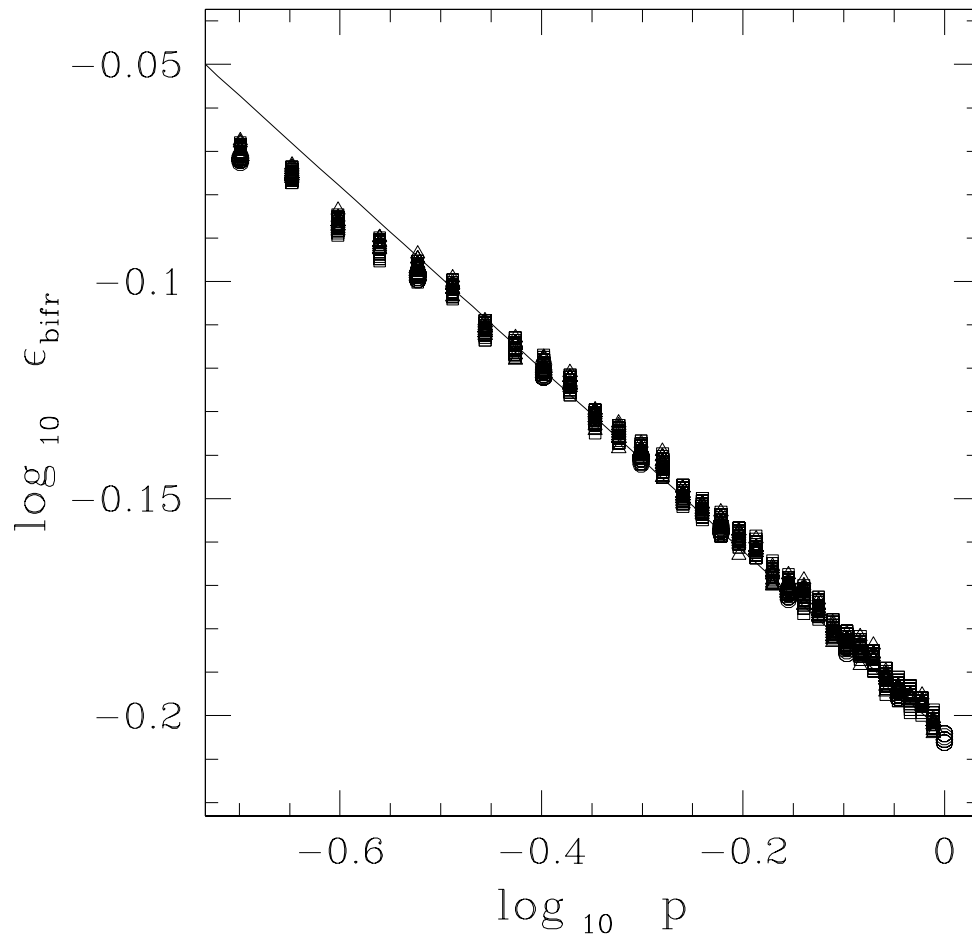


Figure 7: Plot of ϵ_{bifr} (i.e. the value of coupling at which the onset of spatiotemporal synchronization occurs) with respect to fraction of randomly rewired sites p ($0.2 \leq p \leq 1$). The points are obtained from numerical simulations over several different initial conditions, for lattice size $N = 50$, for the case of (a) coupled tent maps (open squares) (b) coupled circle maps (open triangles) and (c) coupled logistic maps (open circles). The solid line displays the best fit straight line for the numerically obtained points.

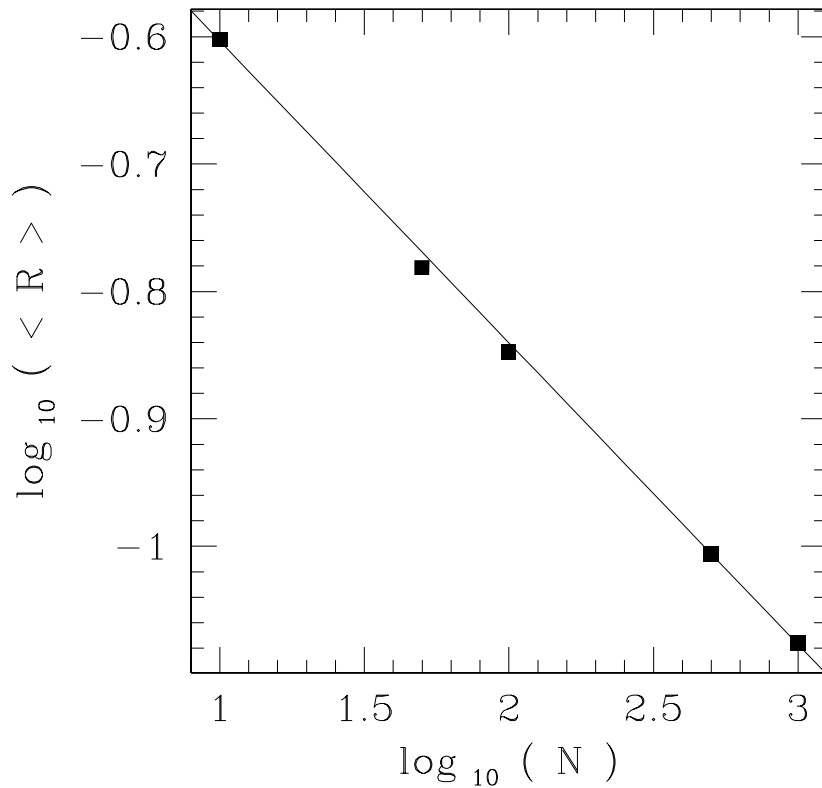


Figure 8: Plot of the average stable range $\langle \mathcal{R} \rangle$ of spatiotemporal synchronisation obtained in the case of static random connections with respect to network size N , for rewired fraction $p = 1$. Here we average \mathcal{R} over 10^4 different realisations of static random connections. The solid line shows the best fit line to the numerically obtained data, indicating clear scaling.